Eur. J. Mineral.
2000, **12**, 1015-1024

Geochronology and geochemistry of single-grain zircons: Simultaneous *in-situ* analysis of U-Pb age and trace elements by LAM-ICP-MS

XIAN-HUA LI[1,2*], XIRONG LIANG[1], MIN SUN[2], YING LIU[1] and XIANGLIN TU[1]

1. Guangzhou Institute of Geochemistry, Chinese Academy of Sciences, Guangzhou 510640, P.R. China

2. Department of the Earth Sciences, The University of Hong Kong, Pokfulam Road, Hong Kong, P.R. China

Abstract: Simultaneous *in-situ* analysis of U-Pb age and 26 trace elements for single-grain zircon using the LAM-ICPMS technique was successfully achieved in this study. The precision of analysis is 1 to 3 % for $^{207}Pb/^{206}Pb$ isotopic ratios, 2 and 8 % for $^{206}Pb/^{238}U$ ratios and 5 to 15 % for most of the other trace elements. The concordia U-Pb and the mean $^{206}Pb/^{238}U$ ages for zircon grain of 1800 Ma to 150 Ma by LAM-ICP-MS spot analysis are in good agreement within analytical errors with the TIMS and SHRIMP results. All zircon grains are uniquely LREE-depleted in chondrite-normalized REE patterns. Zircon formed in mantle-derived magmas is significantly different from that of granitoids with regard to contents of many trace elements (*i.e.*, U, Th, ΣREE, Y, Nb and P) and REE patterns (*i.e.*, Nd/Yb ratio and Ce and Eu anomalies). This combined geochronological and geochemical investigation provides valuable information on timing and genesis of zircon.

Key-words: zircon, U-Pb geochronology, trace elements, LAM-ICP-MS.

1. Introduction

Zircon, $Zr[SiO_4]$, is a common U-rich accessory mineral occurring in many types of rocks, and is therefore the principal material used for U-Pb isotopic dating. Over the last two decades, great achievements in U-Pb zircon dating techniques have been made. These techniques include chemical separation of U and Pb from a single zircon grain, which requires a total procedure Pb-blank of less than 5 picograms (*e.g.*, Krogh, 1982), thermal evaporation of a single zircon grain in thermal ionization mass spectrometry (*e.g.*, Kober, 1986), and *in-situ* micro-spot analysis by sensitive high-resolution ion microprobe (SHRIMP, *e.g.*, Compston *et al.*, 1984), and recently by laser micro-probe inductively coupled plasma-mass spectrometry (LAM-ICP-MS, *e.g.*, Fryer *et al.*, 1993; Feng *et al.*, 1993; Hirata & Nesbitt, 1995; Li *et al.*, 2000). It has been widely recognized that complex geological histories can produce multiple generation domains in a single zircon crystal. For such complex zircon grains, bulk analysis by traditional TIMS technique usually gives geologically meaningless "mixing ages", and the micro-spot analysis of single zircon crystals at 20-30 μm scale is par-

*E-mail: gzisolab@public.guangzhou.gd.cn

DOI: 10.1127/0935-1221/2000/0012-1015 $ 2.50

ticularly important to zircon geochronology. SHRIMP has proven its great ability to reveal the source of provenance, age of crystallization and time of metamorphic overgrowths, by *in-situ* micro-spot analysis of zircon grains. However, high machine and operating costs hampered its wide application in resolving geological problems. More recently, the LAM-ICP-MS technique of *in-situ* Pb-Pb and U-Pb dating of zircon has been rapidly developed, and it has shown a great potential as a simple and relatively low-cost method in U-Pb zircon geochronology. Meanwhile, in order to interpret the complex history recorded in multiple domains in a single zircon grain, observations of zircon morphology and structure by microphotography and cathodoluminescent photography have become a common practice in zircon studies. Compared to SHRIMP, LAM-ICP-MS is a simple and low-cost micro-spot analytical technique with only slightly poorer analytical precision. With machine cost comparable to TIMS, LAM-ICP-MS does not require dissolution of zircon and chemical separation, and consequently analyses are much simpler and faster, but less accurate. The objective of this study is to develop a method of quick and simultaneous *in-situ* analyses of both U-Pb and Pb-Pb isotopic ages and trace elements for single zircon crystals using the LAM-ICPMS technique. Trace-element analysis of zircon will enhance our understanding of zircon geochemistry and in turn help us with the age interpretation.

2. Analytical method

Five zircon samples from different geological environments, with ages ranging from late Paleoproterozoic (~ 1.8 Ga) to Mesozoic (150 Ma) were chosen for this study. These zircon grains have a large grain size (> 100 μm), are optically clear and free of overgrowths, fractures and inclusions, and have been precisely dated by either TIMS or SHRIMP techniques. Zircon grains were loaded into an epoxy mount, polished to half-grain depth, and then washed using purified 2 % HNO_3 for 3 to 5 min prior to analysis.

The basic instrumentation at the Guangzhou Institute of Geochemistry, Chinese Academy of Sciences used in this study is a Perkin-Elmer Sciex ELAN6000 ICP-MS coupled to a CETAC LSX-100 Laser Probe, which is based on a frequency-quadrupled Nd-YAG UV laser system operating at 266 nm. The spectrometric system of this instrument is composed of a golden-ceramic quadrupole mass analyzer with mass resolution of 0.5 to 1.0 amu and a discrete electron multiplier with a deadtime of 60 ns and < 1 cps of noise level. All analyses have been done with a pulse repetition rate of 5 Hz and a beam energy of ~ 1 mJ/pulse. In this case, the vertical ablation rate ranges from 0.3 μm/s to 0.5 μm/s depending on the hardness of the analyzed zircon grains, with a spatial resolution of 20 to 30 μm in diameter with a depth of approximately 20-40 μm. Consequently, the ablated mass from each analyzed spot ranges from ~ 50 ng to ~ 100 ng, with ~ 0.1 % of ion transmission during the analyzing time of 60-80 seconds. The detailed LAM-ICP-MS operating conditions used in this study are summarized in Table 1. These conditions are mostly similar to those for solution analysis, with somewhat higher nebulizer flow rate and AC rod offset voltage optimized for ^{206}Pb in order to increase the sensitivity (Li *et al.*, 2000). To get an optimal ion-lens setting for each mass peak measured and to decrease the matrix effect resulting partly from the ICP and the interface, three peaks of ^{45}Sc, ^{139}La, and ^{232}Th were selected to optimize the autolens voltages.

Rapid peak hopping with dwell times of 40 ms for ^{204}(Pb, Hg), ^{206}Pb, ^{207}Pb, ^{238}U, and ^{29}Si, and 20 ms for the other trace elements, and three to four replicate analyses with 25 sweeps constitute an

Table 1. Operating conditions for LAM-ICP-MS used in this study.

Laser Probe:		
Wavelength	266 nm	
Operating mode	Q-switched	
Repetition rate	5 Hz	
Energy	~ 1 mJ/pulse	
pulse duration	5 ns	
Sampling method	Spot ablation	
Ablation size	20-30 × 30 m^2	
Preablation time	5 seconds	
ICP-MS:		
RF power	1000 W	
Plasma gas flow	15 L/min	
Auxillary gas flow	1.2 L/min	
Nebulizer gas flow	1.0 L/min	
Cones	Pt (Sampling), Ni (Skimmer)	
AutoLens voltage	Sc 6.2V, La 7.8V, Th 8.6V	
AC rod offset voltage	-12.4 V	
Mass resolution	0.70 amu (at 10 % peak height)	
Scanning mode	peak hopping	
Dwell time	20-40 ms	
Replicates	3-4	
Instrument background and sensitivity:		
Masses	Gas Background (cps)	Sensitivity (cps/ppm)
^{202}Hg	100±50	
^{204}(Hg+Pb)	40±20	
^{206}Pb	25±10	150-200
^{207}Pb	30±10	150-200
^{238}U	5±5	150-200

average data set. A spot analysis takes about 60 to 80 seconds, including a pre-ablation time of 5 seconds followed by a reading delay of 5 seconds. Isobaric interference of ^{204}Hg overlapping ^{204}Pb was automatically corrected by the internal software in ELAN6000. In our practice, counts of ^{204}Pb during the course of this study vary within ± 5 cps, and the measured $^{206}Pb/^{204}Pb$ ratios, with omission of the minus values, are mostly > 3000 for Precambrian zircon and > 400 for Mesozoic zircon. No common lead correction was performed. The ^{204}Hg interference prohibits the measurement of ^{204}Pb for common Pb estimation (Compston, 1999). The $^{206}Pb/^{238}U$ ages are not very sensitive to the usual amounts of common Pb, but $^{207}Pb/^{206}Pb$ ages are, due to the much lower abundance of radiogenic ^{207}Pb. Prohibition of common Pb correction is therefore an important limitation on the accuracy of zircon ages determined by LAM-ICPMS.

The isotopes free from isobaric interference were selected for measurements of the other trace elements. Oxide and molecular interference were assumed to be negligible because of low oxides yield (*e.g.* $BaO^+/Ba^+ < 0.3$ %, $SmO^+/Sm^+ < 0.5$ %, and $ThO^+/Th^+ < 0.3$ %). High-grade argon gas, carrying away the ablated materials into the ICP-MS, was measured twice to establish a blank prior to starting ablation for each analysis. Limits of detection (LOD) by 3σ method are typically better than 10 to 30 ppb for REE, Nb, Ta, Ba, Hf, Th, and U, 0.1 to 0.3 ppm for Rb, Sr, Y, ^{204}Pb, and ^{207}Pb, about 0.5 ppm for ^{206}Pb, and 5 to 10 ppm for Sc and P.

The mass discrimination factor for the $^{207}Pb/^{206}Pb$ ratio was determined by analyzing glass standard NIST610. The mass discrimination during daily measurements for $^{207}Pb/^{206}Pb$ ratio is commonly less than 1 %. Experiments have shown that U/Pb ablation fractionation during the spot analysis caused by increasing defocussing of the laser beam was a fundamental problem that hampers the precise U/Pb age determination of zircon by LAM-ICP-MS. In order to minimize the U/Pb fractionation during the ablation process, Li *et al.* (2000) adopted a linear-scan ablation technique of LAM-ICP-MS, instead of the conventional spot ablation technique, to maintain constant focussing of the laser beam on the zircon surface. This linear-scan ablation technique is able to achieve precise $^{207}Pb/^{206}Pb$ ages at about 1 % level for Precambrian (> 1000 Ma) zircon and 2-5 % for Mesozoic (156-126 Ma) zircon (Li *et al.*, 2000). Such a linear-scan ablation technique, however, is not suitable for the simultaneous determination of U-Pb and Pb-Pb ages and trace elements because of significant chemical zoning of zircon. Thus, spot ablation has to be carried out. On the other hand, our experiments show that U/Pb fractionation during spot ablation process usually increase with time and sequential depth as a result of defocussing of the laser beam, but significant fractionation in U/Pb usually occurs after 60 to 80 seconds of ablation. Consequently, only the initial (within 60 seconds, occasionally extended to 80 seconds) $^{206}Pb/^{238}U$ values are used for each data spot, which was similar to the observations of Ludden *et al*. (1995). Typical values of the U/Pb fractionation factor obtained using the spot ablation are usually less than 10 %, in contrast to less than 5 % using the linear-scan ablation (Li *et al.*, 2000). Measurements of $^{207}Pb/^{206}Pb$ and $^{206}Pb/^{238}U$ ratios on each spot ablation are evaluated and averaged to yield an individual value and 2σ standard deviation. Accordingly, $^{207}Pb/^{206}Pb$ and $^{206}Pb/^{238}U$ ages for each spot are calculated from the mean values. The concordia ages are calculated for the old zircon with concordant $^{207}Pb/^{206}Pb$ and $^{206}Pb/^{238}U$ ages, whilst only the weighted grand mean $^{206}Pb/^{238}U$ ages are calculated for young zircon. U-Pb and Pb-Pb ages are calculated after Ludwig (1998).

Calibration for element concentrations was performed using the NIST610 as an external standard, which was analyzed three times before and after seven unknowns. To smooth out the signal variations during analysis and the matrix effect between samples, peak intensities, excepting ^{204}Pb, ^{206}Pb, ^{207}Pb and ^{238}U, were normalized to ^{29}Si with the stoichiometrical value of 32.9 wt% SiO_2, considering its constancy in the zircon lattice.

U-Pb isotopic data and age results for five zircon samples are presented in Table 2 and Fig. 1. Table 3 lists the concentrations of 26 trace elements for different zircon samples along with NIST612 for comparison of accuracy and precision of analysis.

3. Results and discussion

3.1 U-Pb ages

NM15

This sample was taken from a pegmatite in Inner Mongolia, China. It contains large (> 5 mm) euhedral igneous zircon grain. Concordant U-Pb and Pb-Pb ages of 1887 ± 2 Ma (age uncertainties

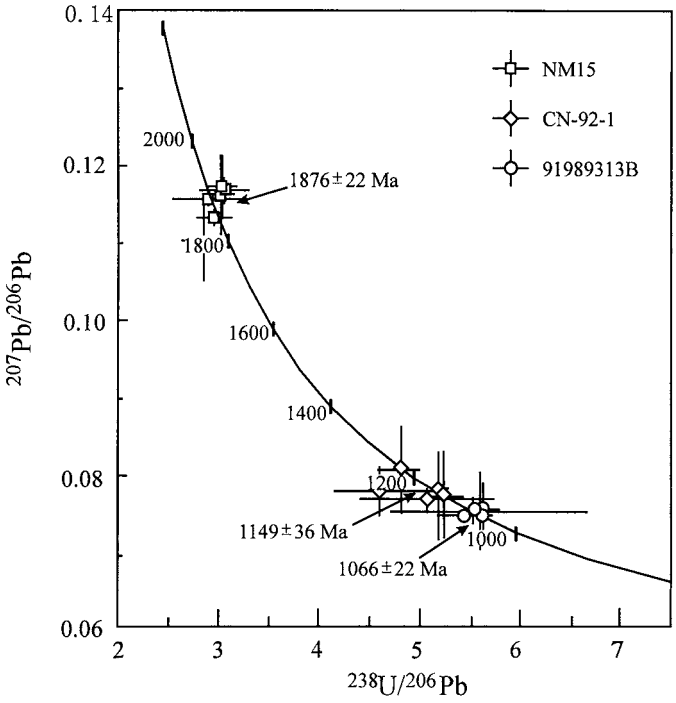

Fig. 1. Tera-Wasserburg $^{238}U/^{206}Pb$ *vs.* $^{207}Pb/^{206}Pb$ concordia plot for zircon samples determined by spot analysis of LAM-ICP-MS.

are quoted at 2σ level in this paper) were obtained by six TIMS analyses of different fragments (Liu *et al.*, 1998). This zircon is now used as our laboratory standard for optimizing the analytical conditions and controlling the mass discrimination of the instrument. Six spot analyses in this study yield concordant $^{206}Pb/^{238}U$ and $^{207}Pb/^{206}Pb$ ages within analytical errors. A concordia age of 1876 ± 21 Ma is then obtained from these concordant $^{206}Pb/^{238}U$ and $^{207}Pb/^{206}Pb$ analyses in the Tera-Wasserburg concordia plot after Ludwig (1998) (Fig. 1 and Table 2), which is in good agreement, within analytical errors, with the TIMS age. Age precision in this study is about ten times poorer than that of TIMS data.

CN-92-1

This sample, taken from a skarn in the Grenville Province, Canada, has been established as a standard with a TIMS $^{207}Pb/^{206}Pb$ age of 1143 ± 2 Ma (Feng *et al.*, 1993). Five spot analyses in this study gave concordant $^{206}Pb/^{238}U$ and $^{207}Pb/^{206}Pb$ ages within analytical errors, and thus average a concordia age of 1149 ± 36 Ma (Fig. 1 and Table 2). This age is identical within analytical errors with the TIMS age, with a precision eighteen times poorer than that of TIMS result.

91989313B

This sample was taken from a granophyre in the Bell Rock gabboric intrusions of the Giles Complex, central Australia. It contains large euhedral, simply zoned igneous zircon grains which gave a concordant SHRIMP U-Pb age of 1078 ± 3 Ma (Sun *et al.*, 1996). Our spot ablation analysis on four zircon grains yielded tightly concordant $^{206}Pb/^{238}U$ and $^{207}Pb/^{206}Pb$ ages within analytical errors, and consequently a concordant age of 1066 ± 22 Ma (Fig. 1 and Table 2), which is consistent with the SHRIMP age. Precision of this result is about eight times poorer than that of the SHRIMP analysis.

91MS29

This is a charnockite sample taken from the Huai'an Complex of the Huabei Granulite Belt, North China Craton. Three fractions of euhedral pink zircon grains were dated by TIMS, giving slightly discordant $^{206}Pb/^{238}U$ and $^{207}Pb/^{235}U$ ages, but consistent $^{207}Pb/^{206}Pb$ age of 1802 ± 4 Ma (Guo *et al.*, 1994). The zircon grain used in this study has a very low U content (< 20 ppm) and consequently has very low ^{207}Pb. Thus, only the $^{206}Pb/^{238}U$ age was determined by spot ablation

Table 2. U-Pb isotopic data for zircon samples.

Spot	$^{206}Pb/^{204}Pb$	$^{206}Pb/^{238}U \pm 2\sigma$	$^{207}Pb/^{206}Pb \pm 2\sigma$	Age (Ma)*	
				$t_{206/238} \pm 2\sigma$	$t_{207/206} \pm 2\sigma$
NM15					
1	>4000	0.329±0.031	0.1173±0.0086	1830±150	1920±130
2	>6500	0.346±0.084	0.1157±0.0022	1920±400	1891±34
3	>5000	0.328±0.054	0.1167±0.0034	1830±260	1906±52
4	>5000	0.351±0.052	0.1102±0.0106	1940±250	1800±170
5	>3000	0.338±0.040	0.1132±0.0022	1880±190	1851±35
6	>3000	0.331±0.029	0.1162±0.0102	1840±140	1900±160
Concordia age = 1876±22 Ma* (MSWD = 0.84)					
TIMS age = 1887±2 Ma (Liu *et al.*, 1998)					
CN-92-1					
1	>5000	0.208±0.018	0.0806±0.0124	1218±96	1210±300
2	>6000	0.217±0.042	0.0778±0.0064	1270±220	1140±160
3	>2500	0.193±0.012	0.0771±0.0106	1138±65	1120±270
4	>3500	0.197±0.052	0.0768±0.0032	1160±280	1116±83
5	>3000	0.191±0.014	0.0771±0.0106	1127±76	1120±270
Concordia age = 1149±36 Ma* (MSWD = 2.49)					
TIMS age = 1143±2 Ma (Feng *et al.*, 1993)					
91989313B					
1	>5000	0.178±0.010	0.0754±0.0072	1056±55	1080±190
2	>7000	0.184±0.018	0.0747±0.0010	1089±98	1060±27
3	>6000	0.179±0.062	0.0752±0.0032	1060±340	1074±85
4	>6000	0.181±0.042	0.0752±0.0034	1070±230	1074±91
Concordia age = 1066±22 Ma* (MSWD = 0.001)					
SHRIMP age = 1078±3 Ma (Sun *et al.*, 1996)					
91MS29					
1	>5000	0.324±0.036		1810±180	
2	>3000	0.316±0.034		1770±170	
3	>4000	0.315±0.037		1770±180	
4	>3500	0.327±0.050		1820±240	
5	>3000	0.318±0.024		1780±120	
Weighted average		0.319±0.015		1785±146*	
TIMS age = 1802±4 Ma (Guo *et al.*, 1994)					
Siberian					
1	>600	0.0216±0.0048		138±30	
2	>500	0.0253±0.0032		161±20	
3	>400	0.0233±0.0048		148±30	
4	>550	0.0233±0.0060		148±38	
5	>900	0.0236±0.0068		150±43	
6	>700	0.0240±0.0032		153±20	
Weighted average		0.0239±0.0017		152±22*	
SHRIMP age = 150±4 Ma (Griffin *et al.*, 1999)					

Note: Age calculated using decay constants 1.55125×10^{-10} yr^{-1} for ^{238}U and 9.8485×10^{-10} yr^{-1} for ^{235}U. Concordia ages are calculated from the concordant $^{206}Pb/^{238}U$ and $^{207}Pb/^{206}Pb$ analyses in the Tera-Wasserburg concordia plot, and the MSWD values are given for the weighted-mean analysis concordance without decay-constant errors after Ludwig (1998).
*Errors on the concordia and weighted mean ages are quoted at the 2σ level.

analysis. Five spot analyses give a mean $^{206}Pb/^{238}U$ age of 1785 ± 146 Ma, which is indistinguishable within analytical uncertainty with the TIMS result. The large age uncertainty is due to the relatively low counts of ^{206}Pb and ^{238}U.

Siberian

This zircon is from the Lomonosova carbonatite from the Ary-Mastakh region of the Siberian platform. Five SHRIMP analyses were made on a

Table 3. Trace-element results for zircon samples by LAM-ICP-MS (average data for several analytical points).

Sample	NIST612		J18		NEB291*		91989313B		84-YG-79		NM15		91500*		AKZ*		Siberian		CN-92-1		91MS29	
Rock type	Conc.	SD	Granite	SD	Granite	SD	Granophyre	SD	Granodiorite	SD	Pagmatite	SD	Syenite	SD	Kimberlites	SD	Carbonatite	SD	Skarn	SD	Charnockite	SD
P	46.4	15.5	1805	1651	2270	2190	927	121	382	157	52	16			65.8	20.9	88	11	22	8	116	13
Sc	42.5	1.7	253	42	576	351	214	24	298	40	225	19					360	26	235	14	237	20
Rb	29.6	1.3	3.5	2.5			3.1	1.5	0.3	0.4	0.3	0.1					0.12	0.03	0.19	0.06	0.22	0.10
Sr	73.5	0.9	2.0	0.8	59	49	2.5	1.3	0.4	0.3	0.17	0.04	0.1	0.04	0.8	3.1	0.18	0.09	0.16	0.03	0.10	0.02
Y	43.0	2.8	1259	314	14500	11300	3843	169	762	367	326	12	146	22	38.8	18.7	124	4	579	48	383	64
Nb	42.4	1.1	4.7	1.3	318	241	111	25	2.0	0.9	4.7	0.5	1.0	0.1	3.6	2.1	6.7	3.2	0.4	0.04	1.2	0.14
Ba	37.2	1.3	2.0	1.3	65	50	4.9	2.7	1.3	1.3	2.0	0.8			0.9	2.9	0.66	0.18	0.35	0.09	0.37	0.24
La	37.0	1.6	18	2	29.4	21	0.94	0.47	0.27	0.18	0.02	0.01	0.2	0.1	0.37	1.58	0.07	0.02	0.30	0.07	0.06	0.02
Ce	38.3	1.5	75	16	162	107	41	1	4.3	2.1	4.1	1.6	2.5	0.5	1.3	2	0.99	0.1	4.5	0.5	17	1
Pr	39.9	2.6	9	2	25.7	21	0.56	0.16	0.21	0.19	0.05	0.01	0.1	0.1	0.42	1.81	0.10	0.02	0.13	0.03	0.14	0.02
Nd	36.6	2.0	40	15	133	114	6.3	0.7	2.7	1.2	0.83	0.27	0.4	0.1	0.7	1.2	1.26	0.12	1.7	0.7	2.0	0.4
Sm	39.6	2.5	16	4	126	103	5.6	0.1	3.4	1.2	1.04	0.33	0.5	0.2	0.9	1.3	1.5	0.2	1.8	0.6	3.3	1
Eu	36.6	2.1	1.1	0.5	6.2	2.8	0.37	0.09	0.23	0.16	0.05	0.02	0.3	0.1	0.67	1.56	0.87	0.3	0.8	0.1	0.72	0.25
Gd	41.0	1.4	35	7	338	269	39	2	21	4	5.6	1.0	2.1	0.3	2.2	1.3	4.4	0.5	8.7	0.9	12	3
Tb	39.1	1.5	10	2			18	1	5.2	1.0	1.84	0.21					1.3	0.1	3.3	0.6	3.2	0.6
Dy	37.6	1.7	111	20	1570	1250	287	13	62	24	24	2	11.2	2.1	5.2	2.6	14	1	43	6	35	6
Ho	41.2	2.0	40	3			101	6	22	11	8.5	0.3	4.7	0.6	1.5	0.8	3.8	0.1	14	1	11	2
Er	41.4	1.9	214	76	456	341	586	36	105	57	47	2	25.3	3.6	5	2.3	15	1	90	8	55	8
Tm	40.0	1.6	41	10			138	10	23	12	9.1	0.9					2.9	0.2	21	2	11	1
Yb	39.4	1.7	387	104	3520	2580	1251	108	204	112	77	9	62	7	6.1	2.8	23	1	206	18	97	13
Lu	38.4	1.6	71	29	553	395	225	11	37	20	14	2	13.9	1.8	1.1	0.6	4.0	0.2	41	3	18	2
Hf(%)	39.2[#]	1.6	1.02	0.13	1.38	0.78	0.98	0.14	0.93	0.09	1.0	0.1	0.60		1.39	0.17	0.70	0.11	0.65	0.06	0.72	0.05
Ta	42.9	1.6	1.8	0.4	38.5	46	33	5	0.74	0.26	1.5	0.1	0.5	0.1	3	1.2	4.6	0.5	0.07	0.02	0.26	0.04
Pb	40.8	3.8	142	121	17.2	11	885	129	106	46			2.5	0.7	1.9	5.3	6.7	2.3	68	6	16	8
Th	38.7	2.1	310	181	1790	1290	967	158	79	28	290	36	29.8	4.7	3.3	2.1	12	7	66	5	21	3
U	37.7	1.4	1111	730	1890	1630	3365	337	301	95	967	95	85	14	10.9	5.5	39	11	214	30	18	3

*Data from Belousova *et al.* (1998). NEB291, 91500, and AKZ are the average of 7, 4, 28 measurements, respectively. Results of the other samples are the average of 5 measurements.
[#] Hf content of NIST612 is in ppm

single large zircon fragment, and yielded a mean $^{206}Pb/^{238}U$ age of 150 ± 4 (2σ) Ma (Griffin *et al.*, 1999). Seven spot analyses of same zircon fragment by LAM-ICP-MS gave a mean $^{206}Pb/^{238}U$ age of 152 ± 18 Ma. This age is consistent with the SHRIMP result, with a precision being about five times poorer.

In summary, all the $^{207}Pb/^{206}Pb$ and $^{206}Pb/^{238}U$ ages determined by LAM-ICP-MS in this study are in good agreement, within analytical uncertainties, with results of TIMS or SHRIMP. The precision is 1 to 3 % for $^{207}Pb/^{206}Pb$ isotopic ratios, 2 to 8 % for $^{206}Pb/^{238}U$. The precision of the calculated concordia ages from the concordant $^{206}Pb/^{238}U$ and $^{207}Pb/^{206}Pb$ analyses for Precambrian zircons ranges from 1.1 % to 3.1 % (Table 2). $^{206}Pb/^{238}U$ age precision for a Mesozoic carbonatite zircon in this study is 14 %, which is about five times poorer than that (2.7 %) by SHRIMP (Griffin *et al.*, 1999) and linear-scan LAM-ICP-MS (Li *et al.*, 2000), due to relatively large variations of the measured $^{206}Pb/^{238}U$ ratios and the small amount of data acquisition in the LAM-ICP-MS spot analysis.

3.2 Trace elements

Twenty-six trace elements were simultaneously determined with the U-Pb ages for the above five zircon samples and another two granitoid zircon grains (samples J18 and 84-YG-79). For the sake of simplicity, the studied zircon samples are divided into mantle-derived and crustal zircon in terms of their host rocks. The mantle-derived zircon includes kimberlite, carbonatite and syenite zircon, whilst the crustal zircon includes granitoid (granite, granodiorite and granophyre), metamorphic (skarn and charnockite) and pegmatite zircon (Table 3). Precision of trace elements in zircons by single spot ablation analysis is typically 5 %-15 % (RSD) for most trace elements, but up to 20 to 40 % for a few trace elements (such as La, Pr, Eu, *etc*.) with concentrations close to the limits of detection (LOD). Apart from low contents for most trace elements in zircon, chemical zoning is likely the cause of large deviations (Pearce *et al.*, 1992). Quantitative results for twenty-six trace elements were obtained through calibration of relative element sensitivities using an external NIST-610 glass standard. To evaluate the matrix effect and accuracy of the data, standard glass NIST-612 was determined five times as an unknown sample, of which the results, with an analytical precision of 3 to 6 %, show a good agreement with the compilation values (Pearce *et al.*, 1997), except P close to its LOD.

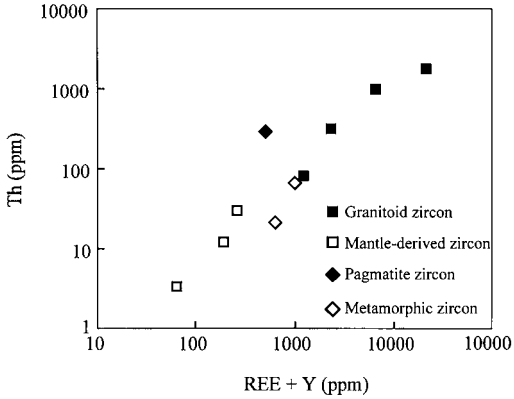

Fig. 2. Plot of REE+Y *vs*. Th in zircon grains from different rock types, showing a positive correlation. REE+Y contents are low (< 300 ppm) for mantle-derived and high (1252-21419 ppm) for granitoid zircon, respectively.

3.2.1 Rare earth elements (REE)

REE composition varies in a broad range and the REE patterns are the most diagnostic feature for different genetic zircon samples. Total REE contents are low for mantle-derived zircon, *i.e.*, less than 50, 100 and 135 ppm for zircon from kimberlite (Belousova *et al.*, 1998), carbonatite and syenite, respectively (Table 3). In contrast, granitoid zircon has much higher total REE contents, ranging from several hundred to several thousand ppm. REE+Y and Th show a good positive correlation (Fig. 2).

All zircon samples are uniquely LREE-depleted in the chondrite-normalized REE patterns and show HREE-increasing patterns (Fig. 3). The depletion of the LREE for zircon can be quantified by the chondrite-normalized $(Nb/Yb)_{cn}$ values, following Belousova *et al.* (1998), because La and Pr contents are very low and Ce shows an anomaly. The kimberlite and carbonatite zircon has gently sloping REE patterns with $(Nd/Yb)_{cn}$ values of 0.02-0.04, whilst syenite zircon shows a very steep slope with $(Nd/Yb)_{cn}$ values of 0.002. Most crustal zircon samples are characterized by a steep slope with $(Nd/Yb)_{cn}$ values of 0.002-0.007, except highly evolved granitic zircon (J18 and NEB291) displaying a gentle slope with $(Nd/Yb)_{cn}$ values of 0.013-0.036.

Ce and Eu anomalies vary significantly for different zircon samples (Fig. 3). Mantle-derived zircon has less pronounced Ce and Eu anomalies. Kimberlite zircon is characterized by the absence of significant positive Ce and negative Eu anoma-

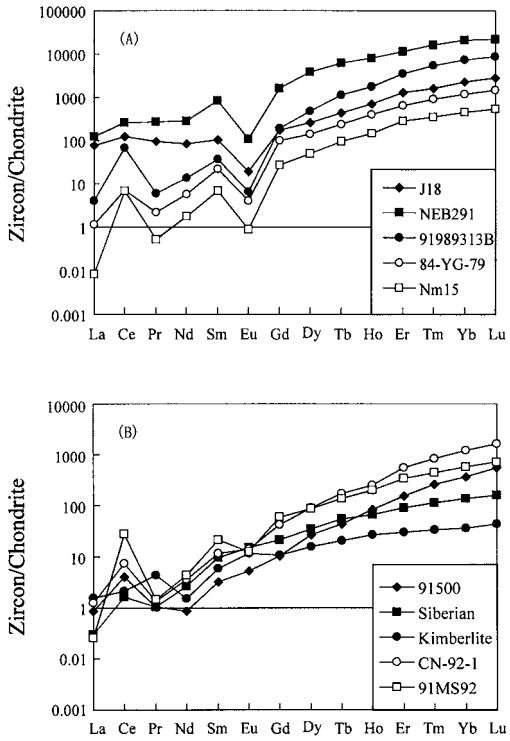

Fig. 3. Chondrite-normalized REE patterns for (A) the granitoid zircon samples, and (B) the mantle-derived and metamorphic zircon samples.

lies, or even slightly negative Ce and positive Eu anomalies (Belousova *et al.*, 1998). Carbonatite and syenite zircon has a slightly positive Ce anomaly (Ce/Ce* = 2.3-4.1) and a very small negative Eu anomaly (Eu/Eu* = 0.76-0.97). In contrast, crustal zircon has variable pronounced Ce and Eu anomalies, with Ce/Ce* = 1.3-30 and Eu/Eu* = 0.05-0.5. A positive Ce anomaly is connected with the presence of Ce^{4+} reflecting the high redox conditions, whilst a negative Eu anomaly is mainly caused by preferential entry of Eu^{2+} ions into plagioclase. Ce/Ce* and Eu/Eu* show a good negative correlation, with mantle-derived and granitoid zircon following different trends (Fig. 4). Mantle-derived zircon has both less pronounced Ce and Eu anomalies, indicating that they crystallized at low redox conditions. In contrast, granitoid zircon has pronounced positive Ce and negative Eu anomalies, suggesting that it crystallized from magmas by plagioclase-separation at high redox conditions.

On the Eu/Eu* *vs.* Th plot (Fig. 5), mantle-derived zircon shows a negative correlation with

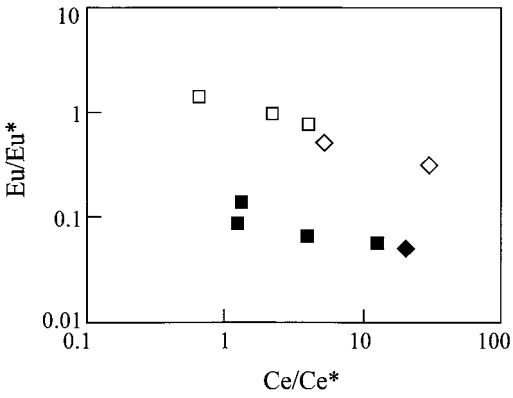

Fig. 4. Eu/Eu* *vs.* Ce/Ce* plot of zircon from different sources. Symbols as in Fig. 2.

low Th contents and high Eu/Eu* ratios, whilst granitoid zircon displays unique low Eu/Eu* ratios over a wide range of Th contents. Skarn and charnokite zircon has Eu/Eu* ratios and Th contents in between those of mantle-derived and granitoid zircon.

3.2.2 Other trace elements

Large-ion lithophile elements (LILE, Rb, Sr and Ba) are very low and do not exceed 5 ppm in most zircon, except in the highly evolved granitoid zircon NEB291 which has exceptionally high Sr and Ba contents of ~ 60 ppm.

The Nb content is generally low, and does not exceed 10 ppm for mantle-derived and metamorphic zircon. But the Nb content varies significantly in granitoid zircon, ranging from 2 to 318 ppm. Overall, Ta is positively correlated with Nb

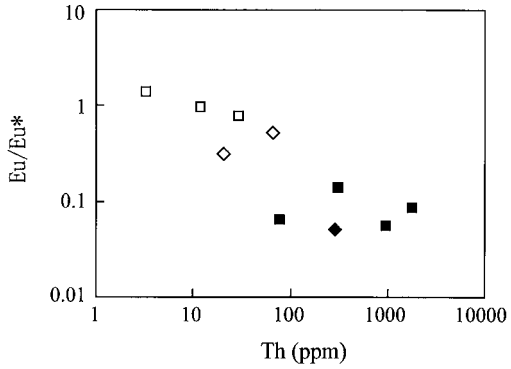

Fig. 5. Eu/Eu* *vs.* Th plot of zircon from different sources. Symbols as in Fig. 2.

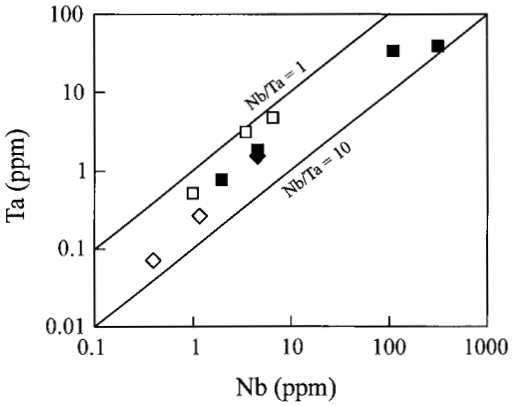

Fig. 6. Ta *vs*. Nb plot of zircon from different sources. Symbols as in Fig. 2.

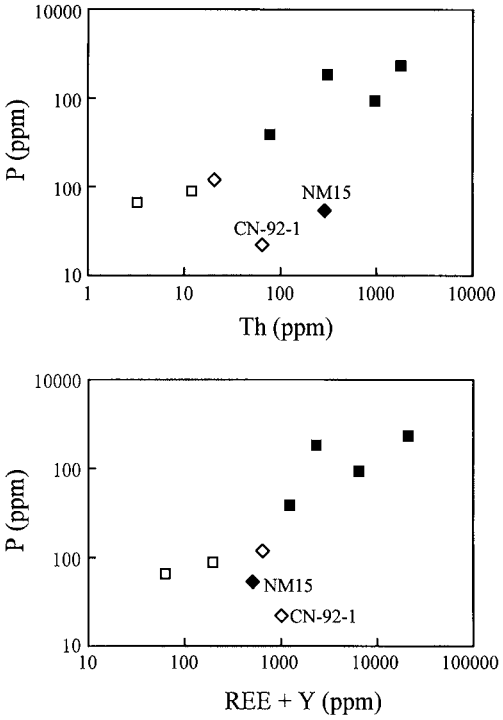

Fig. 7. P *vs.* Th (a) and REE+Y plots of zircon from different sources, showing positive correlations. Note that skarn and pegmatite zircon has exceptionally low P contents and deviate from the positive trends. Symbols as in Fig. 2.

(Fig. 6), with Nb/Ta ratios varying from 1.2 to 8.3, significantly lower than the condritic value of ~ 17 (Sun & McDonough, 1989) and the Nb/Ta ratio of ~ 12 for most granitoids (Harris *et al.*, 1986). Mantle-derived zircon with low Nb and Ta has low Nb/Ta ratios of 1.2-2.0, whilst granitoid and metamorphic zircon samples with variable Nb and Ta contents have relatively higher Nb/Ta ratios of 2.6-8.3. A low Nb/Ta ratio in zircon relative to their environment is likely a common feature, indicating that Ta could enter preferentially into the Hf (Zr) site.

Phosphorus ranges from about 20 to 2270 ppm for different zircon samples, and is positively correlated with Th and REE+Y (Fig. 7). Skarn and pegmatite zircon has exceptionally low P contents and deviate from the positive trends. In general, mantle-derived (kimberlite and carbonatite) zircon has low P contents of < 100 ppm, whilst P varies from hundreds to thousands of ppm for granitoid zircon.

It should be noted that the geochemical features for different zircon samples are generalized from a small number of samples, which require further investigations.

4. Concluding remarks

Simultaneous *in-situ* analysis of U-Pb and Pb-Pb ages and twenty-six trace elements for single-grain zircons using the LAM-ICPMS technique was carried out in this study. Although age precision by this method is about ten to twenty times poorer than that by TIMS and SHRIMP, the concordia U-Pb ages for old zircon (> 1000 Ma) and the $^{206}Pb/^{238}U$ age for Mesozoic zircon are in good agreement within analytical uncertainties, with their ages obtained by TIMS or SHRIMP.

Precision of trace elements in zircon by single spot ablation is generally 5 %-15 % for most trace elements, but up to 20 to 40 % for a few trace elements with concentrations close to the LOD. Trace-element contents, such as U, Th, REEs, Nb, Ta and P, vary in a broad range for different zircon samples. Mantle-derived zircon generally has low contents of most trace elements, *i.e.*, < 100 ppm (mostly < 40 ppm) for U, < 30 ppm for Th, < 100 ppm for ΣREE, < 150 ppm for Y, < 10 ppm for Nb and < 100 ppm for P. They are diagnostically characterized by the absence of significant positive Ce and negative Eu anomalies. In contrast, granitoid zircon usually has high and variable contents for most trace elements, up to several hundred or thousand ppm for U, Th, ΣREE, Y and P. Granitoid zircon shows a unique negative Eu anomaly, but a variable positive Ce anomaly. Thus, mantle-derived and granitoid zircon samples are clearly

different in trace-element geochemistry. The simultaneous *in-situ* analysis of U-Pb age and trace elements for single-grain zircons has significant implications for enhancing our understanding of zircon geochemistry and in turn help us in age interpretation.

Acknowledgment: We wish to thank Drs. R. Feng, S.-S. Sun, P.D. Kinny and H.X. Zhang for generously providing us with their precisely dated zircons. XHL thanks the Croucher Foundation of Hong Kong for a six-month visiting fellowship to the Department of Earth Sciences, The University of Hong Kong. The paper has benefited from the helpful and constructive comments of Drs. Ken Ludwig and Riccardo Petrini and an anonymous reviewer. This work was co-supported by the National Natural Science Foundation of China (Grant Nos. 49725309 and 49903006), Chinese Academy of Sciences (Grant Nos. KZ952-J1-408 and 981105) and a Hong Kong University CRCG grant.

References

Belousova, E.A., Griffin, W.L., Pearson, N.J. (1998): Trace element composition and cathodoluminescence properties of southern African kimberlitic zircons. *Mineral. Mag.*, **62**, 355-366.

Compston, W. (1999): Geological age by instrumental analysis: the 29th Hallimond Lecture. *Mineral. Mag.*, **63**, 297-311.

Compston, W., Williams, I.S., Myer, C. (1984): U-Pb geochronology of zircons from lunar breccia 73217 using a sensitive high mass-resolution ion microprobe. *J. Geophys. Res.*, **89B**, 525-534.

Feng, R., Machado, N., Ludden, J. (1993): Lead geochronology of zircon by LaserProbe-Inductively Coupled Plasma Mass Spectrometry (LP-ICPMS). *Geochim. Cosmochim. Acta*, **57**, 3479-3486.

Fryer, B.J., Jackson, S.E., Longerich, H.P. (1993): The application of laser ablation microprobe-inductively coupled plasma-mass spectrometry (LAM-ICP-MS) to *in situ* (U)-Pb geochronology. *Chemical Geol.*, **109**, 1-8.

Griffin, W.L., Ryan, C.G., Kaminsky, F.V., O'Reilly, S.Y., Natapov, L.M., Win, T.T., Kinny, P.D., Ilupin, I.P. (1999): The Siberian Lithosphere Traverse: Mantle terranes and the assembly of the Siberian Craton. *Tectonophysics*, **310**, 1-35.

Guo, J., Zhai, M., Li, Y., Yan, Y., Zhang, W. (1994): Isotopic ages and their tectonic significance of metamorphic rocks from middle part of the early Precambrian granulite belt, North China Craton. *in* "Geological Evolution of the Granulite Terrrain in North Part of the North China Craton", X. Qian, and R. Wang (eds.), Seismological Press, Beijing, 130-144 (in Chinese with English abstract).

Harris, N.B.W., Pearce, J.A., Tindle, A.G. (1986): Geochemical characteristics of collision-zone magmatism. *in* "Collision Tectonics", M.P. Coward, & A.C. Pies, (eds.), Geol. Soc. Spec. Publ., **19**, 67-81.

Hirata, T. & Nesbitt, R.W. (1995): U-Pb isotope geochronology of zircon: Evaluation of the laser probe-inductively coupled plasma mass spectrometry technique. *Geochim. Cosmochim. Acta*, **59**, 2491-2500.

Kober, B. (1986): Whole-grain evaporation for $^{207}Pb/^{206}Pb$-age investigations using thermal ion mass spectrometry, and implications to zirconology. *Contrib. Mineral. Petrol.*, **96**, 63-71.

Krogh, T.E. (1982): Improved accuracy of U-Pb zircon ages by the creation of more concordant system using an air abrasion technique. *Geochim. Cosmochim. Acta*, **46**, 637-649.

Li, X.-H., Liang, X.-R., Sun, M., Guan, H., Malpas, J.G. (2000): Precise $^{206}Pb/^{238}U$ age determination on zircons by laser ablation microprobe-inductively coupled plasma-mass spectrometry. *Chemical Geol.*, in print.

Liu, H.C., Zhu, B.Q., Zhang, Z.X. (1998): Single-grain zircon dating by LAM-ICPMS. *Chi. Sci. Bull.*, **43**, 1103-1106 (in Chinese).

Ludden, J.N., Feng, R., Gauthier, G., Stix, J. (1995): Application of LAM-ICPMS analysis to minerals. *Can. Mineral.*, **33**, 419-434.

Ludwig, R.K. (1998): On the treatment of concordant uranium-lead ages. *Geochim. Cosmochim. Acta*, **62**, 665-676.

Pearce, N.J.G., Perkins, W.T., Abell, I., Duller, G.A.T., Fuge, R. (1992): Mineral microanalysis by laser inductively coupled plasma mass spectrometry. *J. Anal. At. Spectrom.*, **7**, 53-57.

Pearce, N.J.G., Perkins, W.T., Westgate, J.A., Gorton, M.P., Jackson, S.E., Neal, C.R., chenery, S.P. (1997): A compilation of new and published major and trace element data for NIST SRM 610 and NIST SRM 612 glass reference materials. *Geostand. Newsl.*, **21**, 115-144.

Sun S.-S. & McDonough, W. F. (1989): Chemical and isotopic systematics of oceanic basalts: Implications for mantle composition and processes. *in* "Magmatism in the ocean basins", A.D. Saunders & M.J. Norry (eds.), Geological Society [London] Special Publication **42**, 313-345.

Sun, S.-S., Sheraton, J.W., Gilkson, A.Y., Stewart, A.J. (1996): A major magmatic event during 1050-1080 Ma in central Australia, and an emplacement age for the Giles Complex. *AGSO Research Newsletter*, **24**, 13-15.

Received 16 July 1999
Modified version received 6 April 2000
Accepted 27 Avril 2000